Rheol Acta (2012) 51:441–450
DOI 10.1007/s00397-011-0614-6

ORIGINAL CONTRIBUTION

Scaling and mesostructure of Carbopol dispersions

Iris A. Gutowski · David Lee · John R. de Bruyn · Barbara J. Frisken

Received: 15 July 2011 / Revised: 24 November 2011 / Accepted: 9 December 2011 / Published online: 18 January 2012

Abstract Rheological measurements were performed on aqueous dispersions of two commercial crosslinked polymer microgels, Carbopol Ultrez 10 and Carbopol ETD 2050, prepared over a wide range of concentration and pH. For all concentrations studied, both the yield stress and the elastic modulus initially increased dramatically with pH and displayed broad peaks at intermediate pH. This is consistent with the onset of jamming of the Carbopol particles due to a rapid increase in particle size caused by osmotic swelling in the presence of NaOH. Scaling of both yield stress and elasticity with concentration was observed only at higher concentrations, which we believe indicates a change from a percolated structure at low volume fractions to a space filling network of compressed particles at high volume fractions. This model is supported by confocal microscopy of fluorescently dyed Carbopol dispersions.

Keywords Microgel · Carbopol · Yield stress · Elastic modulus · Viscoelasticity · Rheology

Introduction

Complex fluids are a fascinating class of materials that exhibit unusual flow properties. Yield-stress fluids are a particularly interesting example. These materials flow when subjected to a shear stress greater than a threshold value, referred to as the yield stress σ_0, but maintain their form and do not flow when the stress is less than σ_0. The ability of such fluids to resist shear makes them useful for a variety of applications; examples include mayonnaise, toothpaste, shaving cream, and concrete. Recently, it has been suggested that a distinction should be made between thixotropic yield-stress fluids, which display a time-dependent viscoelasticity, and "ideal" yield-stress fluids, which do not (Bonn and Denn 2009).

Carbopol microgels are an example of near-ideal yield-stress fluids (Moller et al. 2009; Putz and Burghelea 2009). Carbopol is the trade name of a family of microgels made of highly crosslinked poly(acrylic acid) that are used in a wide variety of industrial applications (Muramatsu et al. 2000; Noveon Pharmaceuticals 2002). Carbopol dispersions are transparent and, even at very low concentration, display a significant yield stress and high elasticity. Their rheological properties can be tuned by varying both pH and concentration and are relatively insensitive to temperature. Carbopol has been used as a model material for investigations of properties of yield-stress fluids (Bonn and Denn 2009; Putz and Burghelea 2009), as well as many problems in fluid dynamics, including bubble dynamics (Sikorski et al. 2009), the settling of particles (Tabuteau et al. 2007), and the formation of cavities by impellers (Amanullah et al. 1998).

Rheological studies of Carbopol and similar microgels have shown that properties such as concentration and crosslink density determine where they lie on the spectrum between entangled linear polymers and non-interacting hard spheres, with higher crosslink densities and lower concentrations making the system more like

I. A. Gutowski · D. Lee · B. J. Frisken (✉)
Department of Physics, Simon Fraser University, Burnaby, British Columbia, Canada
e-mail: frisken@sfu.ca

J. R. de Bruyn
Department of Physics and Astronomy, University of Western Ontario, London, Ontario, Canada

the latter (Steeneken 1989; Carnali and Naser 1992; Naé and Reichert 1992; Borrega et al. 1999). In the 1970s, Taylor and Bagley studied the viscosity of Carbopol varieties 940 and 941 and similar microgels over a range of concentration and pH (Taylor and Bagley 1974, 1975, 1977). They noted two distinct regimes in the concentration-dependence of the viscosity: a linear increase at low concentrations, and a steeper power law increase above a critical concentration. Based on this work, they argued that Carbopol dispersions consist of highly swollen deformable particles that become space-filling above a critical concentration. Later work by Carnali and Naser investigated the effect of crosslink density (Carnali and Naser 1992). They found that the less-crosslinked Carbopol 941 became space filling at lower concentrations than the more highly crosslinked Carbopol 940 and estimated the crosslink density from the rheological measurements.

Microrheology studies support this picture of a viscous fluid at low concentrations and a space filling paste at high concentrations, but suggest a third regime at intermediate concentrations. Oppong and de Bruyn (2011) analyzed the diffusion of tracer particles in Carbopol ETD 2050 at pH 6 over a concentration range $0.01 \leq c \leq 1.0$ wt.%. At low concentrations, the tracer particles diffused freely in a purely viscous rheological environment. At the highest concentration, the particles became strongly confined and little motion was observed. At intermediate concentrations, however, two populations of particles were observed: one that was diffusive and a second, which grew in significance as the concentration increased, that moved in an increasingly viscoelastic environment. A bulk yield stress was measured at intermediate and high concentrations. These results were interpreted as indicating that Carbopol is a suspension at low concentrations, has a percolated structure containing pools of solvent at intermediate concentrations, and has a space-filling structure composed of compressed gel particles at high concentrations.

It has also been shown that pH has a dramatic effect on the rheological properties of Carbopol suspensions (see, e.g., Kim et al. 2003). Carbopol is a polyelectrolyte gel that swells due to a net outward osmotic pressure in the presence of ions (Borrega et al. 1999). Many previous studies of Carbopol have been carried out at neutral pH as this is where yield stress and elasticity tend to be highest and least sensitive to pH (Ketz et al. 1988; Hernández et al. 1998). In this paper, we investigate the rheological behavior of Carbopol over a broad range of pH and concentration. While earlier studies focused on Carbopols 940 and 941 (Taylor and Bagley 1975; Ketz et al. 1988; Curran et al. 2002; Kim et al. 2003; Piau 2007), in the present work we examine Carbopols Ultrez 10 and ETD 2050, which are faster wetting and easier to disperse analogs of 940 and 941, respectively (Noveon Pharmaceuticals 2002). These newer varieties are easier to hydrate, less prone to forming lumps, and less viscous in the pH-unmodified state, features which allow for easier and more consistent sample preparation (Desai et al. 1992; Hernández et al. 1998; Noveon Pharmaceuticals 2002). We examine the dependence of the yield stress and elastic modulus on pH and concentration and supplement our rheological results with images obtained by confocal microscopy to gain information about the development of a yield stress in soft materials.

Experimental

Sample preparation

Carbopols Ultrez 10 and ETD 2050 were obtained from Noveon Pharmaceuticals in powder form. Samples with c ranging from 0.05 to 0.5 wt.% for Ultrez 10 and 0.1 to 5 wt.% for ETD 2050 were prepared by slowly dispersing the appropriate amounts of powder in distilled, deionized, filtered water. This was done by creating a gentle vortex in a large beaker with a magnetic stir bar and adding powder in small increments to the center of the vortex. The mixture was covered and stirred for several days to ensure that the Carbopol was fully hydrated, as confirmed by the absence of visible aggregates.

These dispersions were then divided and small amounts of 20 wt.% NaOH solution were added to obtain samples with a range of pH values. After adding the base, the dispersions were gently agitated with a vortexer and then allowed to equilibrate. We found that it took several hours for the pH to stabilize. This was due to a dramatic increase in local viscosity that occurred with the addition of NaOH, which strongly hindered diffusion of the base through the material. We also found that we needed to leave the digital pH probe (Fisher Scientific Calomel Electrode) in the dispersions for at least 20 min to obtain a stable reading. Samples with pH ranging from the unmodified value of 2.3 to 3.8, depending on concentration, up to pH 11 were prepared. We were careful to avoid overshooting the desired pH, as adding acid to correct the pH leads to charge screening, which can have quite dramatic effects on the viscosity (Ketz et al. 1988). After measuring the pH, we centrifuged the samples at 1,000 rpm to eliminate bubbles.

Rheology

All rheometric measurements were performed using an Ares RHS strain-controlled rheometer equipped with a cone and plate tool. The cone was 5 cm in diameter and had a cone angle of 0.04 radians. Fine sandpaper was glued to both the plate and the outer part of the cone to prevent wall slip (Magnin and Piau 1990). The tool was surrounded by a housing in which the atmosphere was saturated with water vapor to minimize evaporation from the sample. A temperature-controlled circulating water bath was used to keep the samples at a temperature of 25°C. We waited several minutes for each sample to equilibrate after it was loaded, then presheared it at a shear rate of 1 s^{-1} for 30 s followed by a waiting period of 30 s to place it in a reproducible initial state. Oscillatory shear measurements were performed at fixed frequency of 1 rad/s as a function of strain amplitude to determine the extent of the linear viscoelastic regime. On the basis of these measurements, a strain amplitude of 1% was used for small-amplitude oscillatory shear experiments to determine the elastic and viscous moduli, G' and G'', respectively, as a function of frequency. We also measured the flow curve—the stress as a function of shear rate—by applying steady shear and measuring the resulting torque.

A few samples at the low end of the pH and concentration ranges were too fluid to be measured with our rheometer. We were not able to obtain flow curves for Ultrez 10 at $c = 0.05$ wt.% below pH 4.5, 0.1 wt.% below pH 4 and for ETD 2050 at 0.1 wt.% below pH 3.8. We were also unable to obtain viscoelastic moduli as a function of applied strain for Ultrez 10 at 0.05 wt.% below pH 5 and above pH 9, 0.1 wt.% below pH 4.3, and 0.2 wt.% below pH 4, and for ETD 2050 at 0.1 wt.% below pH 4.3.

Confocal microscopy

We directly imaged Carbopol samples using confocal fluorescence microscopy. The Carbopol particles were stained by adding 1 μL 0.5 M Acridine Orange, a cationic dye, to 7 g of sample. Due to its charge, the dye was readily absorbed by the pH-unmodified Carbopol. The samples were stirred for several days prior to imaging to ensure the dye was fully absorbed. The stained gels were placed between a slide and cover slip and imaged using a Nikon A1R Confocal Fluorescence Microscope operating at an excitation wavelength of 488 nm. Unfortunately, adding even small amounts of NaOH to the solution caused the dye to leach out of the particles into the surrounding fluid, substantially reducing the contrast in images of the pH-modified samples.

Results

The majority of the data presented in this section were obtained from measurements on Carbopol Ultrez 10. The data for Carbopol ETD 2050 were qualitatively similar (Gutowski 2010) and are not presented with the same level of detail to avoid redundancy. Our results for the yield stress of ETD 2050 as a function of concentration and pH have previously appeared in Lee et al. (2011). ETD 2050 and Ultrez 10 have different crosslink densities, and we compare their behavior towards the end of this section. Finally, we discuss the scaling of the rheological properties of these materials with concentration.

A plot of stress as a function of shear rate for several concentrations of Ultrez 10 neutralized to pH 7 is shown in Fig. 1a. The lowest shear rate is set by the capabilities of our rheometer, and the highest by instabilities which expel the sample from the rheometer

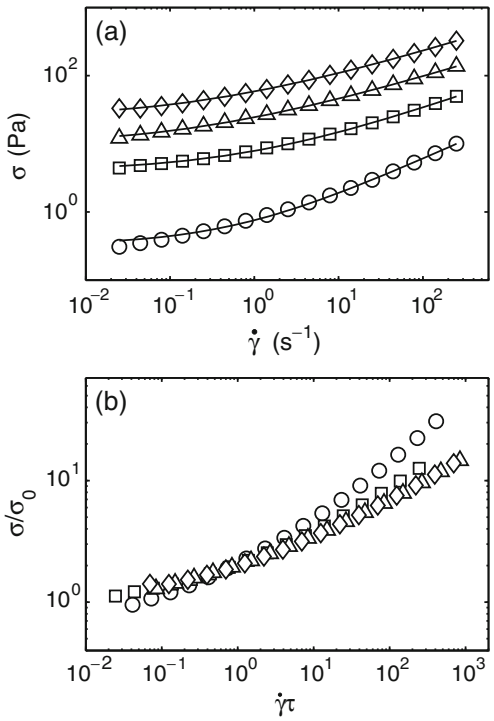

Fig. 1 **a** Stress as a function of shear rate for Carbopol Ultrez 10 neutralized to pH 7. The *curves* are fits of Eq. 1 to the data. **b** Stress scaled by the yield stress plotted as a function of shear rate multiplied by the time constant τ. The data are for concentrations $c = 0.05$ wt.% (*circles*), 0.1 wt.% (*squares*), 0.2 wt.% (*triangles*), and 0.5 wt.% (*diamonds*)

tool. For all cases where flow curves could be measured for this material, the stress approaches a concentration-dependent yield stress at low shear rates. The yield stress σ_0 was determined by fitting the Herschel–Bulkley model,

$$\sigma = \sigma_0 \left[1 + (\tau\dot{\gamma})^n\right] \quad (1)$$

to the data, where σ_0, the power-law exponent n, and the time constant τ were used as fitting parameters. Previous studies have shown that Eq. 1 provides a good description of the flow curve of Carbopol (Kim et al. 2003; Sikorski et al. 2009). It fits our data extremely well in most cases, although small deviations from the fit are seen for the least viscous suspensions, as observed in the data for 0.05 wt.% Ultrez 10 at pH 7 shown in Fig. 1a. In Fig. 1b we show the same data with the stress scaled by the yield stress σ_0 and plotted as a function of the scaled shear rate $\tau\dot{\gamma}$. Data for the two highest concentrations, $c = 0.2\%$ and 0.5%, collapse onto a single curve when plotted in this form, the data for $c = 0.1\%$ show a slight deviation at high $\tau\dot{\gamma}$, while the low concentration data deviate from this curve at both high and low $\tau\dot{\gamma}$. This data is representative of flow curves for Ultrez 10 at other pH. The flow curves for ETD 2050 were also similar, with the exception of dispersions at the lowest concentrations and pH that did not have a measurable yield stress. In particular, the flow curves for ETD 2050 at higher concentrations also collapsed when plotted as in Fig. 1b.

The parameters obtained from the fits of the Herschel–Bulkley model to the Ultrez 10 data are plotted as a function of pH in Fig. 2. The yield stress is very small (<0.1 Pa) for the most fluid samples. As the pH is increased, the yield stress increases by as much as a factor of 300 to a maximum at pH 6, then decreases slowly as the pH is raised further. The broad maximum in yield stress as a function of pH seen in Fig. 2a is observed for all concentrations for both versions of Carbopol. At any given pH, σ_0 increases monotonically with concentration. The time constant τ, shown in Fig. 2b, is approximately 1 s. While there appears to be a trend to larger τ at larger pH, the scatter and uncertainty in these data prevent us from identifying a significant systematic variation of τ with either pH or concentration. The exponent n plotted in Fig. 2c decreases from around 0.8 at low pH to between 0.4 and 0.6 for pH > 5. The values of n obtained at high pH are in agreement with values of approximately 0.5 obtained from previous studies of microgels (Cloitre et al. 2003; Kim et al. 2003; Sikorski et al. 2009). For Ultrez 10, n tends to decrease with concentration at a given pH, approaching a constant value at high concentration; Fig. 3 shows this trend at pH 7. The Herschel–Bulkley exponent n for ETD 2050 also fell within the range $0.4 < n < 0.6$ for pH > 5. In this case there is a tendency for n to increase slightly with concentration at a given pH, but n still approaches a constant value at high concentrations. Data for ETD 2050 at pH 8 are also shown in Fig. 3.

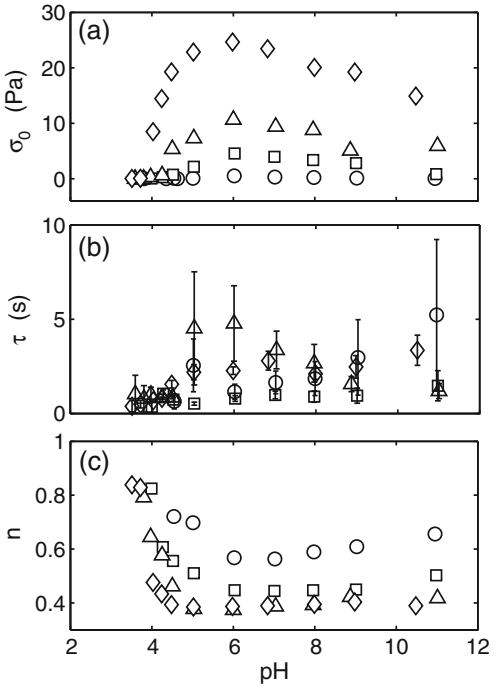

Fig. 2 **a** Yield stress σ_0, **b** time constant τ , and **c** Herschel–Bulkley exponent n determined from fits of our data to Eq. 1, plotted as a function of pH for Carbopol Ultrez 10 at concentrations $c = 0.05$ wt.% (*circles*), 0.1 wt.% (*squares*), 0.2 wt.% (*triangles*), and 0.5 wt.% (*diamonds*). Uncertainties in the parameters that are larger than the symbols are shown as *error bars*

Typical results for both G' and G'' as functions of the amplitude of the oscillatory strain γ are shown in

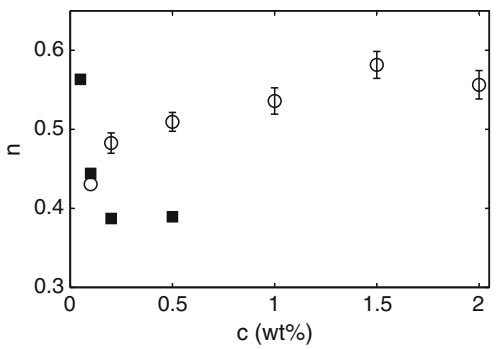

Fig. 3 The Herschel–Bulkley exponent n plotted as a function of concentration for Ultrez 10 at pH close to 7 (*squares*) and for ETD 2050 at pH close to 8 (*circles*)

Fig. 4a for 0.2% Ultrez 10 at pH 7. At low γ, the elastic modulus is approximately 10 times the viscous modulus. For $\gamma \leq 1\%$, G' and G'' are independent of strain amplitude and the material is in the linear viscoelastic regime. Around $\gamma = 10\%$, the elastic modulus begins to roll off, whereas the viscous modulus reaches a maximum and then decreases. For $\gamma > 100\%$, G'' is larger than the elastic modulus. The moduli intersect roughly at the frequency where G'' reaches its maximum. All samples for which data were obtained showed this behavior.

Measurements of G' and G'' as functions of frequency were performed at $\gamma = 1\%$, within the linear viscoelastic regime. Results for 0.2 wt.% Ultrez 10, pH 7 are shown in Fig. 4b. The elastic modulus is essentially constant and substantially larger than the viscous modulus at all frequencies measured. G'' shows a shallow minimum around $\omega = 0.2$ rad/s, suggesting the presence of slow, glassy dynamics (Sollich 1998). This behavior is typical of many soft materials (Sollich et al. 1997), as discussed below. All samples showed similar behavior, and the frequency of the minimum in G'' is roughly independent of concentration and pH.

The plateau value of G' is a good measure of the overall elasticity of the system (Barnes et al. 1989). The values of G' at 1 rad/s are shown in Fig. 5. Like σ_0, G' exhibits a peak as a function of pH for all concentrations studied, and in most cases this peak occurs as the same pH as the peak in σ_0 shown in Fig. 2a. At the highest concentration studied, however, the peak in G' is narrower and occurs at lower pH than the peak in the yield stress, perhaps due to electrostatic interactions between the microgels at high c.

σ_0 and G' for the two different varieties of Carbopol at 0.1, 0.2, and 0.5 wt.% are compared in Fig. 6a and b,

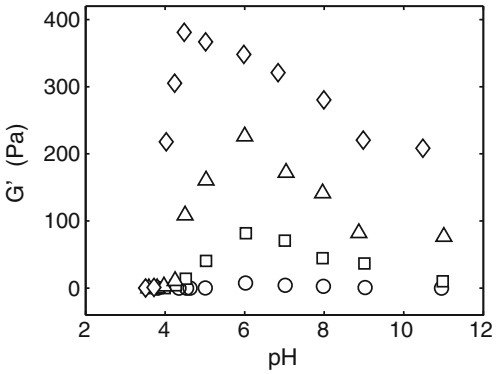

Fig. 5 The elastic modulus G' at $\omega = 1$ rad/s plotted as a function of pH for Carbopol Ultrez 10 at concentrations $c = 0.05$ wt.% (*circles*), 0.1 wt.% (*squares*), 0.2 wt.% (*triangles*), and 0.5 wt.% (*diamonds*)

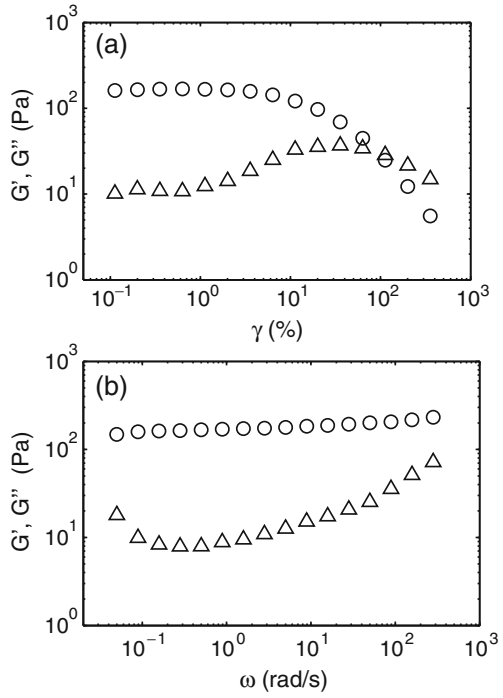

Fig. 4 **a** Plot of the viscous and elastic moduli as functions of strain amplitude at a frequency of 1 rad/s for 0.2 wt.% Carbopol Ultrez 10 at pH 7. **b** G' and G'' plotted as functions of frequency at $\gamma = 1\%$. The *circles* represent the elastic modulus and the *triangles* the viscous modulus

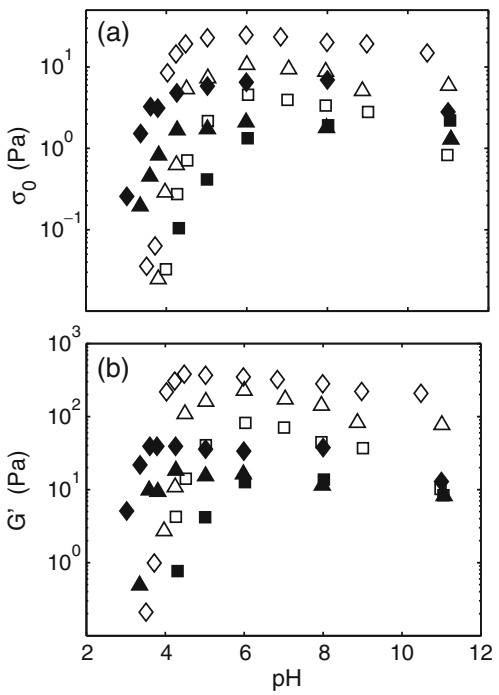

Fig. 6 **a** Yield stress, and **b** elastic modulus, plotted as a function of pH for Ultrez 10 (*open symbols*) and ETD 2050 (*filled symbols*). Concentrations are $c = 0.1$ wt.% (*squares*), 0.2 wt.% (*triangles*), and 0.5 wt.% (*diamonds*)

respectively. The variation with pH of the yield stress and elastic modulus of ETD 2050 is not as dramatic as for Ultrez 10. At low pH and higher concentrations, both the yield stress and elastic modulus of ETD 2050 are higher than for Ultrez 10, while at intermediate pH, the opposite is true. At a given concentration, the peak value of the yield stress is typically five times greater and the elastic modulus 10 times greater for Ultrez 10 than for ETD 2050.

Figure 7 shows the yield stress and elastic modulus of Ultrez 10 scaled by the concentration and plotted as a function of pH. In both cases the data collapse over the whole pH range for $c \geq 0.2$ wt.% and near the peak for the 0.1 wt.% sample. For the lowest concentration, both scaled quantities fall below the results for the higher concentrations over the full range of pH. Yield stress and elastic modulus data for ETD 2050 showed similar scaling with concentration (Gutowski 2010).

Light scattering studies of ETD 2050 microgels for scattering wave vectors ranging from 0.02 to 25 μm^{-1} have been reported by Lee et al. (2011). These measurements revealed microstructure characterized by two length scales: a longer length scale (> 6 μm) that depends on Carbopol concentration and the amount of NaOH added, and a shorter length scale (≈400 nm) that is independent of sample properties. This is consistent with scattering from microgel particles made up of randomly crosslinked polymers with small regions (each less than 1 part per million of the particle volume) that do not swell when the pH is increased, presumably due to a high local crosslink densities. Scattering studies of Ultrez 10 revealed similar behavior at smaller length scales (Gutowski 2010). However, this product is even more transparent resulting in even lower scattering making small angle scattering studies intractable with available equipment.

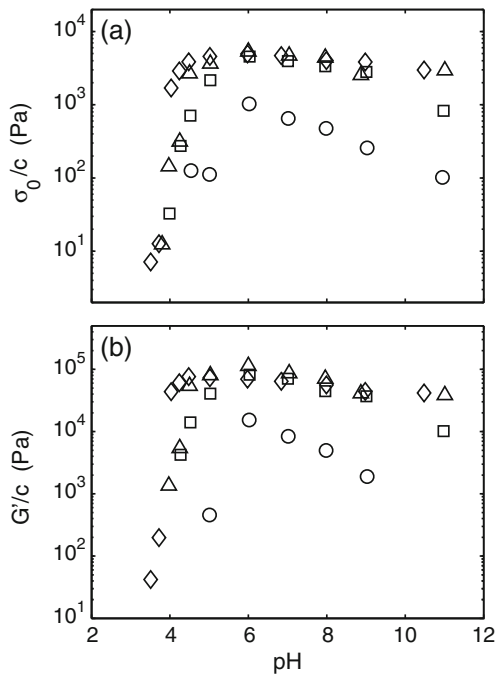

Fig. 7 Plot of **a** yield stress, and **b** elastic modulus, scaled by concentration as a function of pH for samples of Carbopol Ultrez 10 at various concentrations. Concentrations are: 0.05 wt.% (*circles*), 0.1 wt.% (*squares*), 0.2 wt.% (*triangles*), and 0.5 wt.% (*diamonds*)

In order to get further insight into microstructure of this product, we attempted to stain the samples and image them with confocal microscopy. Confocal fluorescence microscopy images of Carbopol microgels stained with Acridine Orange are shown in Fig. 8. These individual images are taken from a stack of images obtained by scanning the focal plane vertically through the sample. They have been contrast-enhanced for display purposes. The suspended gel particles, which have absorbed the fluorescent dye, appear brighter in the images than the surrounding fluid. Although we did not attempt a quantitative size analysis, the images show clearly that the Carbopol particles are quite polydisperse. Figure 8a is an image of unmodified (pH = 3.8) Ultrez 10 at low concentration (0.05 wt.%). A substantial amount of fluid can be seen between the microgel particles. This sample did not have a measurable yield stress. Figure 8b shows unmodified Ultrez 10 (pH 3.5) at a concentration 10 times higher. In this case the image shows that the microgel structure is space filling, and at this concentration the yield stress was 0.04 ± 0.02 Pa. In Fig. 8c we show an image of low concentration Carbopol Ultrez 10 at a pH of approximately 4, only slightly higher than in Fig. 8a. The contrast between the particles and the surrounding fluid in Fig. 8c is significantly lower than in the other images, likely due to the dye leaching out of the particles because of the addition of NaOH. This reduction in contrast got worse as the pH was raised further, making it impossible to image any structure at higher pH. A visual comparison of Fig. 8a and c shows that the microgel particles in Fig. 8c are larger, confirming that raising the pH has caused them to swell. Figure 8d shows an image of ETD 2050 at 0.5 wt.% and pH 3.0. Comparison with Fig. 8b, which shows Ultrez 10 at the same concentration, suggests that the mesostructure is similar in the two materials, but that the particles in ETD 2050 are larger than those in Ultrez 10.

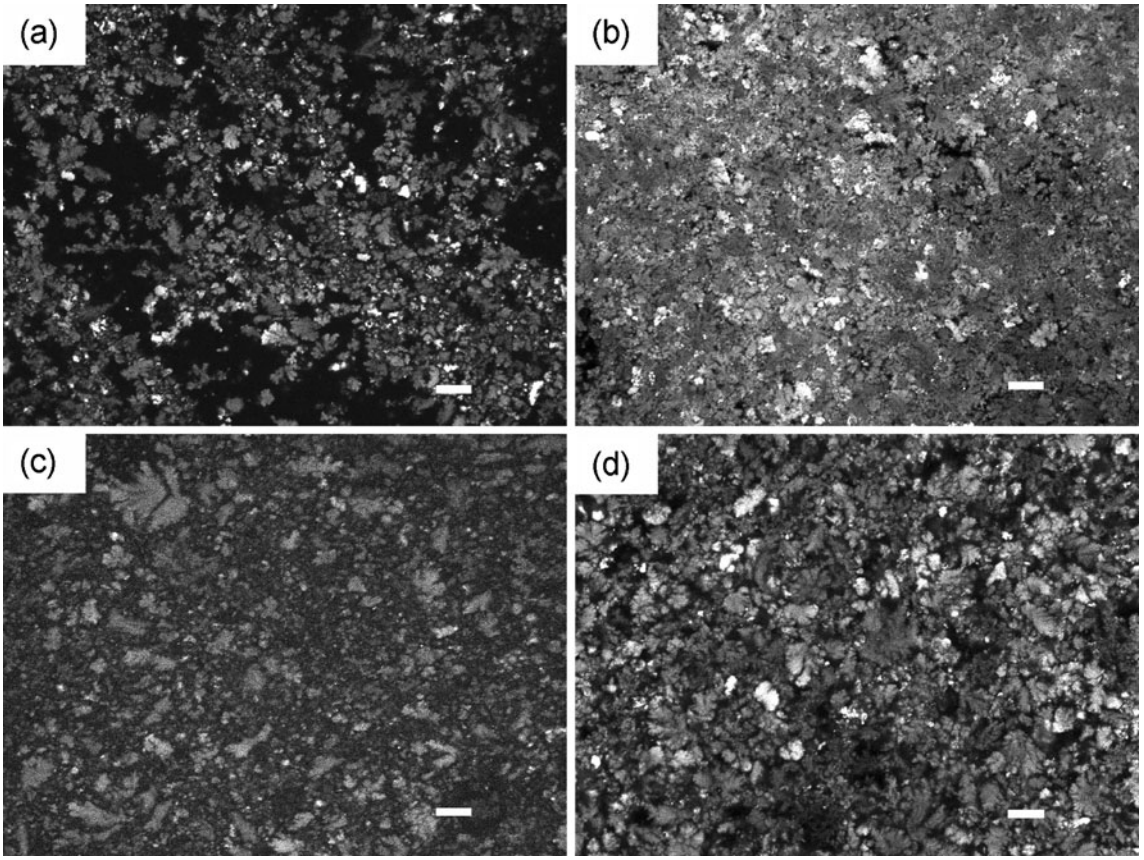

Fig. 8 Confocal images of low pH Carbopol gels dyed with Acridine Orange. The length of the *scale bar* is 20 μm. **a** 0.05 wt.% pH 3.8 (*unmodified*) Ultrez 10. **b** 0.5 wt.% pH 3.5 (*unmodified*) Ultrez 10. **c** 0.05 wt.% Ultrez 10 at pH ≈ 4. **d** 0.5 wt.% pH 3.0 (unmodified) ETD 2050

Discussion

We have carried out a systematic study of the rheological behavior of Carbopol gels ETD 2050 and Ultrez 10 over a wide range of conditions. The flow curves are generally well described by the Herschel–Bulkley model. In oscillatory shear measurements, the elastic modulus dominates the viscous modulus at low strain, and both are independent of strain up to an amplitude of 1%. In the linear regime, both G' and G'' are roughly independent of frequency, with $G''/G' \approx 0.1$. Our results are comparable to those from previous studies of Carbopol 940 and 941 (Curran et al. 2002; Piau 2007; Taylor and Bagley 1974).

The observed rheological behavior is similar to that reported for other disordered systems at higher concentrations, including colloidal glasses (Mason and Weitz 1995), high-concentration compressed emulsions (Mason et al. 1996; Mason and Weitz 1997), polyelectrolyte microgel particles (Cloitre et al. 2003), and star polymers (Erwin et al. 2010). In general, the behavior displayed by these jammed systems is qualitatively consistent with a universal model for soft glassy materials introduced by Sollich et al. (1997) in which the rheological properties of the material are attributed to structural disorder and metastability and thermal fluctuations are not sufficient to drive the material to a globally minimal energy state.

For both varieties of Carbopol, adding base to the dispersion initially increases the yield stress and elastic modulus, although increasing the pH beyond 8 causes both of these quantities to decrease. These observations are consistent with swelling of microgel particles (Saunders and Vincent 1999). The initial increase of the pH causes the acrylic acid groups within the polymer to dissociate. The presence of mobile counter ions results in an increase in the internal osmotic pressure, causing the microgel particles to swell by at least a factor

of 1,000 in volume (Lee et al. 2011; Oppong and de Bruyn 2011). Once the acid becomes fully dissociated, however, further addition of base simply adds ions that screen the fixed charges, decreasing the osmotic pressure and easing the compression of the polymer network. The microgel particles likely deswell in this regime, although Lee et al. (2011) found that they remained too large to be detected in their light scattering measurements. This indicates that any deswelling is much less dramatic than the initial swelling and that the particles do not return to their initial sizes. The slight shrinking of the particles simply relaxes the structure and allows for greater particle motion in response to applied perturbations, resulting in the observed decreases in yield stress and elasticity at high pH. We note that in polyelectrolytes like Carbopol, the degree of neutralization may be more closely related to the polymer microstructure than pH, although pH is a more convenient control parameter from an experimental point of view.

At low pH, the yield stress and elastic modulus of ETD 2050 are substantially higher than the corresponding properties of Ultrez 10, but at intermediate pH they are larger for Ultrez 10 at all concentrations. These observations are consistent with Ultrez 10 being more highly crosslinked that ETD 2050. The swelling capacity of crosslinked polymers varies inversely with their crosslink density (Flory 1953). As the pH is increased at low pH, less-crosslinked particles swell more readily, resulting in higher Carbopol volume fractions and higher values of both yield stress and elastic modulus than achieved in the more-crosslinked material. Once the particles jam together and fill space, however, the properties depend on the elasticity of the individual particles, which is higher for the more-crosslinked material (Flory 1953). The increased elasticity of the more-crosslinked particles gives the bulk material a higher elastic modulus, and this in turn leads to higher values of the yield stress; the more rigid particles cannot deform as easily, and so cannot flow past each other and rearrange (Steeneken 1989; Sollich et al. 1997). Such behavior has been observed previously in space-filling aqueous starch systems which, like Carbopol, consist of swellable, compressible, crosslinked particles (Steeneken 1989). From the ratio of the maximum elastic moduli, we estimate that the crosslink density is a factor of 10 larger in Ultrez 10 than in ETD 2050.

We observe a significant difference in the way that the rheological data scale at low and high concentration of the polymer. At high concentrations, the flow curves have the same Herschel–Bulkley exponent n, and consequently collapse when the stress is scaled by the yield stress and the shear rate by the characteristic time τ, as shown in Fig. 1b. In addition, both the yield stress and the elastic modulus scale with concentration, as shown in Fig. 7. These scalings are not observed at the lowest concentrations measured, and only at intermediate pH for samples of intermediate concentration. We interpret the appearance of this scaling behavior to signal a significant change in the mesostructure of the materials.

Early studies of Carbopol suggested the existence of two structural phases as a function of concentration: a low-concentration viscous fluid and a higher-concentration paste with little interstitial solvent (Taylor and Bagley 1974; Carnali and Naser 1992). In contrast, our data are consistent with three distinct structural phases, as has been observed in other dispersions of soft particles (Mason et al. 1996; Cloitre et al. 2003; Erwin et al. 2010). In these systems, the microstructure is described in terms of the volume fraction φ of the particles, since it is φ that determines the degree of interaction between them. At low volume fractions, the zero-frequency viscosity of these systems increases with φ, diverging at a volume fraction consistent with the glass transition for hard spheres. At this point, the systems develop a significant elasticity and a yield stress, which increase quickly as the number of contact points between the particles increases and the particles start to deform. As the volume fraction approaches 1, the elasticity becomes constant in the cases of the emulsions, or changes approximately linearly with concentration for polyelectrolyte microgels.

In the case of Carbopol, the relationship between $c$and φ is not known in detail, since we have no direct way of measuring the degree of expansion of the microgel particles except at the lowest pH (Lee et al. 2011) and the lowest concentrations (Oppong and de Bruyn 2011). However, it is clear that the volume fraction φ occupied by Carbopol microgels of a given concentration c increases with increasing pH as the microgel particles expand until the particles are fully space-filling, so we will discuss the behavior in these terms. At the lowest concentrations and pH studied, the elasticity and yield stress were not measurable, consistent with a dilute dispersion of swollen microgel particles which behaves as a viscous fluid. For Ultrez 10, this behavior is observed for $c = 0.05$ wt.% below pH 4.5 and for $c = 0.1$ wt.% below pH 4. At intermediate concentration and pH, the elasticity and yield stress increase quickly with pH, indicating the onset of a glassy state where elasticity and yield stress depend on the number of the contact points and deformation of the particles. On further swelling, when the Carbopol volume fraction approaches one and the material consists of compressed microgel particles jammed together in a space-filling arrangement, changes of the elasticity

and yield stress depend on changes in the elasticity of the particles. For Ultrez 10, our results indicate that this occurs for $c \geq 0.2$ wt.% and pH ≥ 5. In the case of polyelectrolyte particles at high concentration, this is dominated by the osmotic pressure due to the concentration of free counterions (Cloitre et al. 2003), which is proportional to the polymer concentration. The fact that the yield stress and elastic modulus follow the same scaling with concentration is consistent with the proportionality between yield stress and modulus expected if the critical strain is roughly independent of concentration. Similar scaling of yield stress and elasticity with concentration was observed in star polymers above the jamming transition (Erwin et al. 2010).

That the intermediate state in Carbopol is characterized by significant void spaces is supported by the fluorescence microsopy images shown in Fig. 8. Our picture is also similar to that proposed by Piau (2007) based on measurements of the yield stress of Carbopol 940 and is consistent with the results of studies of the diffusion of tracer particles in ETD 2050 (Oppong and de Bruyn 2011), which showed the presence of two distinct microrheological regimes at intermediate concentrations—one viscous and the other predominantly elastic—and a single elastic regime at high concentration.

Conclusions

We have studied the viscoelastic properties of aqueous dispersions of two forms of Carbopol, Ultrez 10 and ETD 2050, over a wide range of pH and concentration. As has been observed in other Carbopol varieties, the highest values of yield stress and elastic modulus were found in samples at intermediate pH. At low pH, the yield stress and elastic modulus are higher for ETD 2050, which has a lower crosslink density, but at intermediate and high pH they are higher for Ultrez 10. From our measurements, we estimate that the crosslink density of Ultrez 10 is a factor of 10 higher than that of ETD 2050.

We see evidence of three different mesostructures as the pH is varied. At the lowest concentration and pH, neither Ultrez 10 nor ETD 2050 has a measurable yield stress or elastic modulus. In this regime, the material can be described as a dilute dispersion of relatively noninteracting microgel particles. At intermediate volume fractions, where dispersions are viscoelastic but the yield stress and elasticity do not scale linearly with concentration, Carbopol consists of a percolated structure of gel particles with significant void space. At high volume fraction, i.e., for all pH for high concentration and intermediate pH for the intermediate concentration samples, fits of the Herschel–Bulkley model to the data scale with the value of the yield stress and the characteristic time τ, and the elastic modulus and yield stress each scale with concentration. In this regime, Carbopol can be described as a fully space-filling paste of swollen microgel particles.

Acknowledgements We would like to thank Lester Poon, Sharan Swarup, and Tim Helslip for help with fluorescence microscopy, and Felix Oppong for assistance with rheological measurements. This research was supported by the Natural Science and Engineering Research Council of Canada.

References

Amanullah A, Hjorth SA, Nienow AW (1998) A new mathematical model to predict cavern diameters in highly shear thinning, power law liquids using axial flow impellers. Chem Eng Sci 53:455–469

Barnes HA, Hutton JF, Waters K (1989) An introduction to rheology. Elsevier, Amsterdam

Bonn D, Denn MM (2009) Yield stress fluids slowly yield to analysis. Science 324:1401–1402

Borrega R, Cloitre M, Betremieux I, Ernst B, Leibler L (1999) Concentration dependence of the low-shear viscosity of polyelectrolyte micro-networks: from hard spheres to soft microgels. Europhys Lett 47:729–735

Carnali JO, Naser MS (1992) The use of dilute solution viscometry to characterize the network properties of Carbopol microgels. Colloid Polym Sci 270:183–193

Cloitre M, Borrega R, Monti F, Leibler L (2003) Glass dynamics and flow properties of soft colloidal pastes. Phys Rev Lett 90:068303

Curran SJ, Hayes RE, Afacan A, Williams MC, Tanguy PA (2002) Properties of Carbopol solutions as models for yield-stress fluids. J Food Sci 67:176–180

Desai DD, Hasman DF, Schmucker-Castner JF (1992) Advances in carbomer polymer technology. Cosmet Toilet Manuf Worldw 107:81–94

Erwin BM, Cloitre M, Gauthier M, Vlassopoulos D (2010) Dynamics and rheology of colloidal star polymers. Soft Mater 6:2825–2833

Flory PJ (1953) Principles of polymer chemistry. Cornell University Press, Ithaca

Gutowski IA (2010) The effects of pH and concentration on the rheology of Carbopol gels. MSc Thesis, Simon Fraser University. https://theses.lib.sfu.ca/thesis/etd6172

Hernández MJ, Pellicer J, Delegido J, Dolz M (1998) Rheological characterization of easy-to-disperse (ETD) Carbopol hydrogels. J Dispers Sci Technol 19:31–42

Ketz RJ, Prud'homme RK, Graessley WW (1988) Rheology of concentrated microgel solutions. Rheol Acta 27:531–539

Kim J-Y, Song J-Y, Lee E-J, Park S-K (2003) Rheological properties and microstructures of Carbopol gel network system. Colloid Polym Sci 218:614–623

Lee D, Gutowski IA, Bailey AE, Rubatat L, de Bruyn JR, Frisken BJ (2011) Investigating the structure of a yield-stress polymer gel by light scattering. Phys Rev E 83:031401

Magnin A, Piau J-M (1990) Cone-and-plate rheometry of yield stress fluids. Study of an aqueous gel. J Non-Newton Fluid Mech 36:85–108

Mason TG, Weitz DA (1995) Linear viscoelasticity of colloidal hard sphere suspensions near the glass transition. Phys Rev Lett 75:2770–2773

Mason TG, Weitz DA (1997) Osmotic pressure and visco elastic shear moduli of concentrated emulsions. Phys Rev E 56:2150–3166

Mason TG, Bibette J, Weitz DA (1996) Yielding and flow of monodisperse emulsions. J Colloid Interface Sci 179:439–448

Moller P, Fall A, Chikkadi V, Derks D, Bonn D (2009) An attempt to categorize yield stress fluid behavior. Phil Trans R Soc A 367:5139–5155

Muramatsu M, Kanada K, Nishida A, Ouchi K, Saito N, Yoshida M, Shimoaka A, Ozeki T, Yuasa H, Kanaya Y (2000) Application of Carbopol to controlled release preparations I. Carbopol as a novel coating material. Int J Pharm 199:78–83

Naé HN, Reichert WW (1992) Rheological properties of lightly crosslinked carboxy copolymers in aqueous solutions. Rheol Acta 31:351–360

Noveon Pharmaceuticals (2002) Noveon Polymers Technical Bulletins.

Oppong FK, de Bruyn JR (2011) Microrheology and jamming in a yield-stress fluid. Rheol Acta 50:317–326

Piau J-M (2007) Carbopol gels: elastoviscoplastic and slippery glasses made of individual swollen sponges meso- and macroscopic properties, constitutive equations and scaling laws. J. Non-Newton Fluid Mech 144:1–29

Putz AMV, Burghelea TI (2009) The solid–fluid transition in a yield stress shear thinning physical gel. Rheol Acta 48:673–689

Saunders BR, Vincent B (1999) Microgel particles as model colloids: theory, properties and applications. Adv Colloid Interface Sci 80:1–25

Sikorski D, Tabuteau H, de Bruyn JR (2009) Motion and shape of bubbles rising through a yield-stress fluid. J Non-Newton Fluid Mech 159:10–16

Sollich P (1998) Rheological constitutive equation for a model of soft glassy materials. Phys Rev E 58:738–759

Sollich P, Lequeux F, Hébraud P, Cates ME (1997) Rheology of soft glassy materials. Phys Rev Lett 78:2020–2023

Steeneken PAM (1989) Rheological properties of aqueous suspensions of swollen starch granules. Carbohydr Polym 11:23–42

Tabuteau H, Coussot P, de Bruyn JR (2007) Drag force on a sphere in steady motion through a yield-stress fluid. J Rheol 51:125–137

Taylor NW, Bagley EB (1974) Dispersions or solutions? A mechanism for certain thickening agents. J Appl Polym Sci 18:2747–2761

Taylor NW, Bagley EB (1975) Rheology of dispersions of swollen gel particles. J Polym Sci 13:1133–1144

Taylor NW, Bagley EB (1977) Tailoring closely packed gel-particle systems for use as thickening agents. J Appl Polym Sci 21:113–122